Electronic Supplementary Material (ESI) for Journal of Materials Chemistry A.

Supporting Information

Cryptomelane $K_{1.33}Mn_8O_{16}$ as a Cathode for Rechargeable Aqueous Zinc-ion Batteries

*Krishnakanth Sada, Baskar Senthilkumar and Prabeer Barpanda**

Faraday Materials Laboratory, Materials Research Centre, Indian Institute of Science,

Bangalore, 560012, India

* prabeer@.iisc.ac.in, Phone: +91-08-2293-2783; Fax No: +91-80-2360-7316

Crystallographic information

Lattice parameters from the Rietveld refinement of the $K_{1.33}Mn_8O_{16}$ (*I*4/*m* space group)

a = 9.8633(11) Å

c = 2.86514(28) Å

Volume = 278.73(8) Å^3

Symmetry = Tetragonal

Symmetry space group name H-M = "*I*4/*m*"

Table S1: Atomic positions of the $K_{1.33}Mn_8O_{16}$.

Atoms	x	y	z	Occ.	U_{iso}	Wykoff position
K1	0.0	0.0	0.41979	0.38431	0.06907	4e
Mn1	0.35006	0.16685	0.0	0.96531	0.00139	8h
O1	0.15444	0.20391	0.0	1.00045	0.01327	8h
O2	0.54298	0.16692	0.0	0.91304	0.03215	8h

Table S2: The area ratio of peaks Mn $2p_{3/2}$ and $2p_{1/2}$.

S.No			Area	Ratio
1	Pristine	$2p_{1/2}$	272.4	1.96
		$2p_{3/2}$	535.7	
2	1st discharge	$2p_{1/2}$	381.7	2.08
		$2p_{3/2}$	796.7	
3	1st charge	$2p_{1/2}$	1068.0	1.99
		$2p_{3/2}$	2130.3	
4	15th discharge	$2p_{1/2}$	1450.0	1.92
		$2p_{3/2}$	2797.0	

Table S3: Comparison of the peak positions at (2θ = 12.9 and 18.2) showing shift in the ratio.

	Peak-Position (2θ)	d-spacing (Å)	Counts	Ratio
1st charge	12.96	6.80	3637	
	18.26	4.85	3694	0.985
1st discharge	12.76	6.93	4402	
	18.48	4.79	2026	2.172
15th charge	12.95	6.82	3045	
	18.24	4.83	3250	0.9369
15th discharge	12.52	7.06	6768	
	18.26	4.85	2809	2.409

Table S4: Comparison of prominent studies on α -MnO_2 cathode still date.

Sl. No	Active Material	Discharge product	Morphology	Electrolyte	Capacity (mA h g^{-1})	Reference
1	α-MnO_2	$ZnSO_4[Zn(OH_2)_3]$. xH_2O, MnOOH	Nanofibers	$ZnSO_4$ and $MnSO_4$	(C/5) 285	1
2	α-MnO_2	$ZnMn_2O_4$ and MnOOH	MnO_2 deposited on CFP	$ZnSO_4$ and $MnSO_4$	(0.3C) 290	2
3	α-MnO_2	$ZnMn_2O_4$	Powder	$ZnSO_4$ or $Zn(NO_3)_2$	(0.5C) 210	3
4	α-MnO_2	Zn- birnessite	Nanorods	1M $ZnSO_4$	(C/20) 205	4
5	α-MnO_2	$ZnMn_2O_4$	Nanorods	$ZnSO_4$	233	5
6	KMn_8O_{16}	$ZnK_{1-x}Mn_8O_{16}$	Nanorods	$ZnSO_4$ and K_2SO_4	(1C) 77	6
7	**$K_{1.33}Mn_8O_{16}$**	**Zn- birnessite**	**Nano particles**	**$ZnSO_4$ and $MnSO_4$**	**(C/10) 312**	**This work**

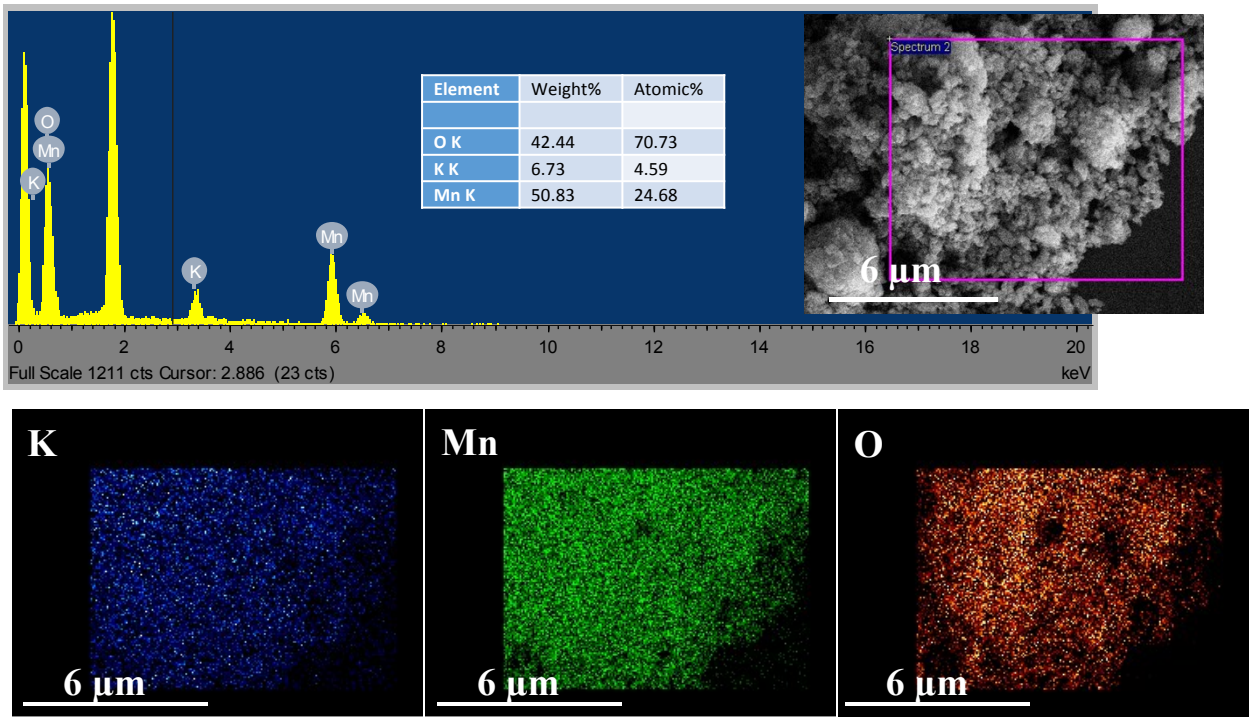

Figure S1: EDS and elemental mapping of the $K_{1.33}Mn_8O_{16}$ showing uniform distribution of constituent elements.

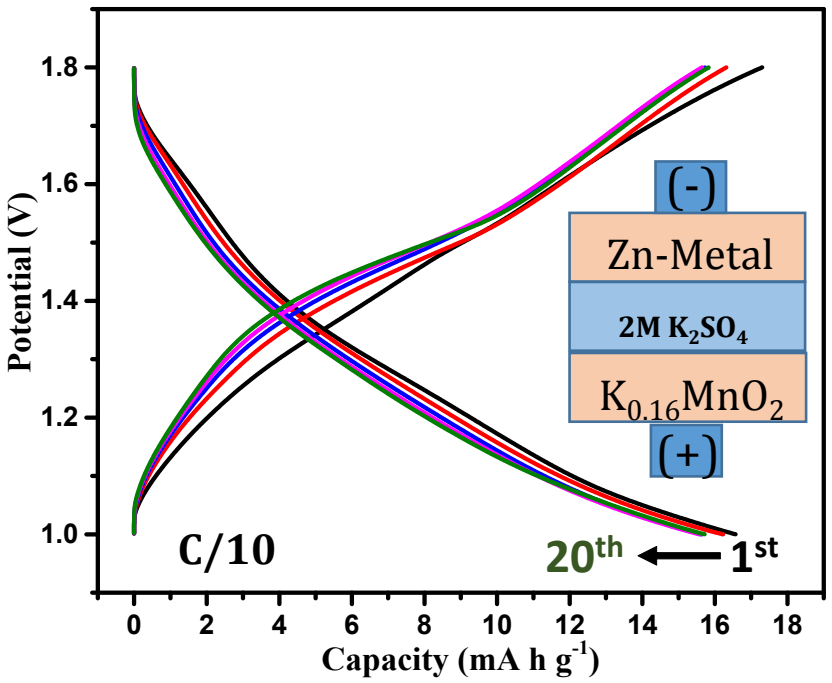

Figure S2: Galvanostatic charge/ discharge (GCD) cycles of $K_{1.33}Mn_8O_{16}$ in 2M K_2SO_4 electrolyte. (Inset) Schematic presentation of the cell assembly.

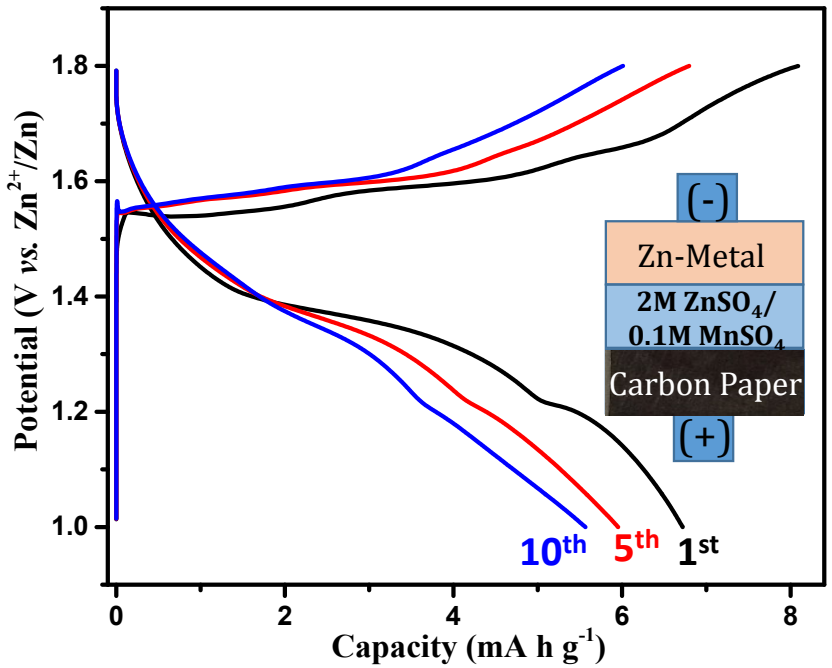

Figure S3: Galvanostatic charge/ discharge (GCD) cycles of carbon paper without active material in 2M $ZnSO_4$ in 0.1M $MnSO_4$ additive electrolyte. (Inset) Schematic presentation of the cell assembly.

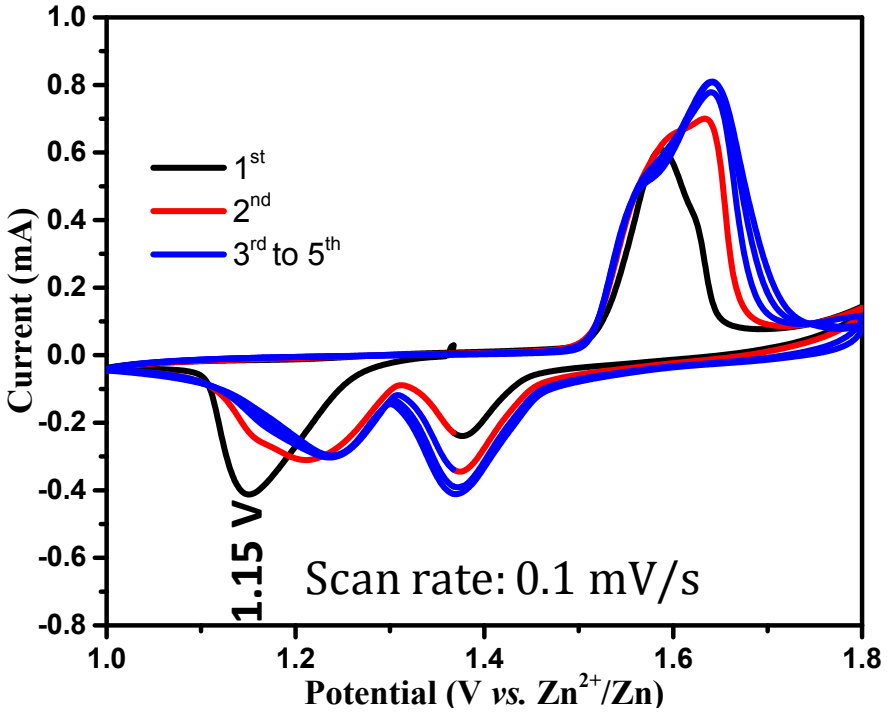

Figure S4: Cyclic voltammetry (CV) curves recorded in the potential window of 1-1.8 V at a scan rate of 0.1 mV/s.

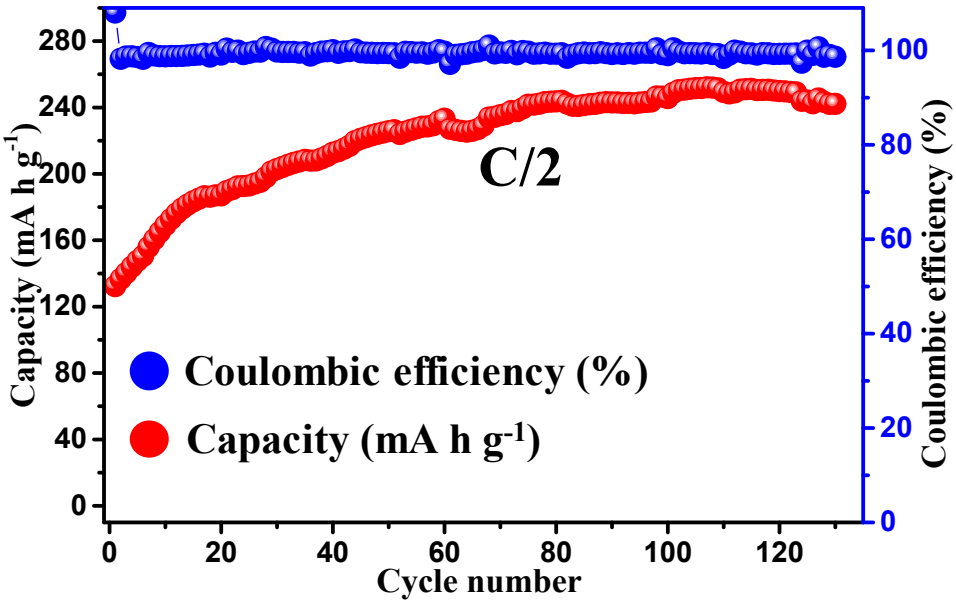

Figure S5: Cycling stability for 130 cycles at the current rate of C/2.

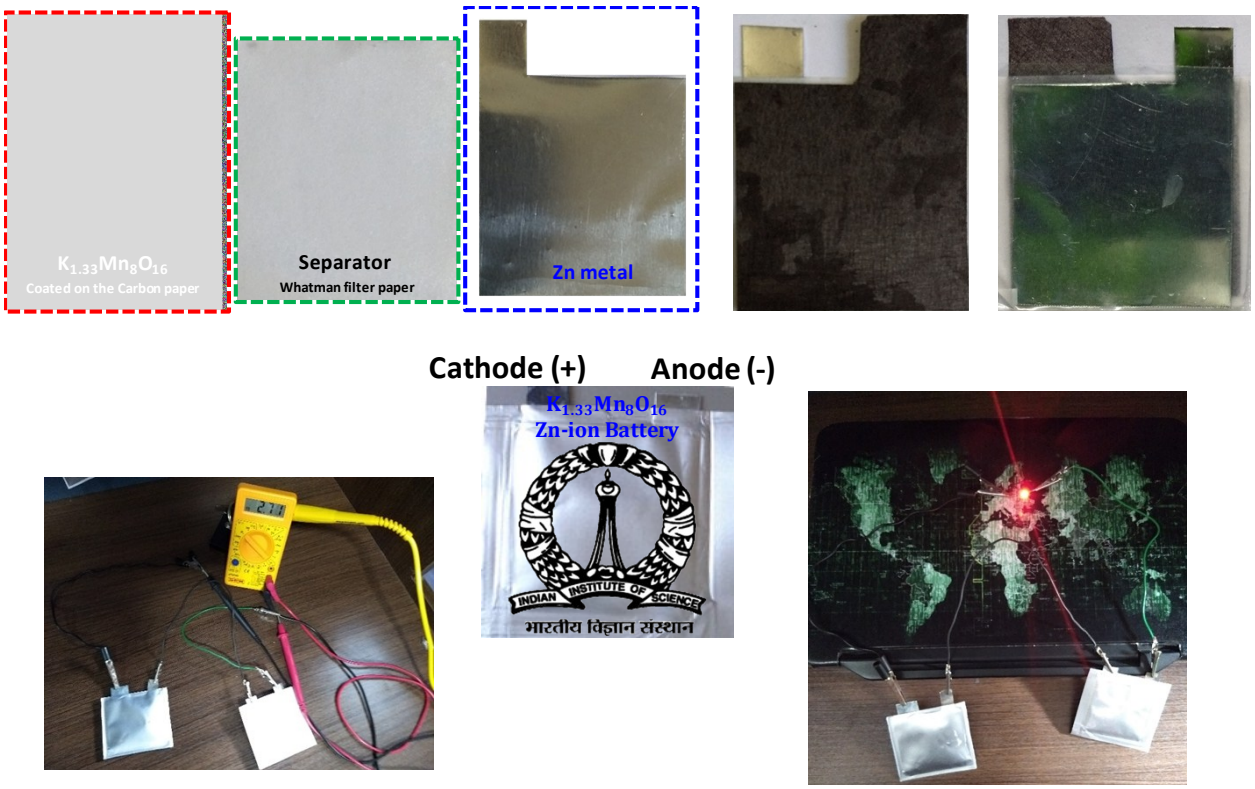

Figure S6: The pouch cell components and different stages of the assembly. The OCV of the two cell is 2.71 V. The assembled pouch cell was tested successfully to light a red LED.

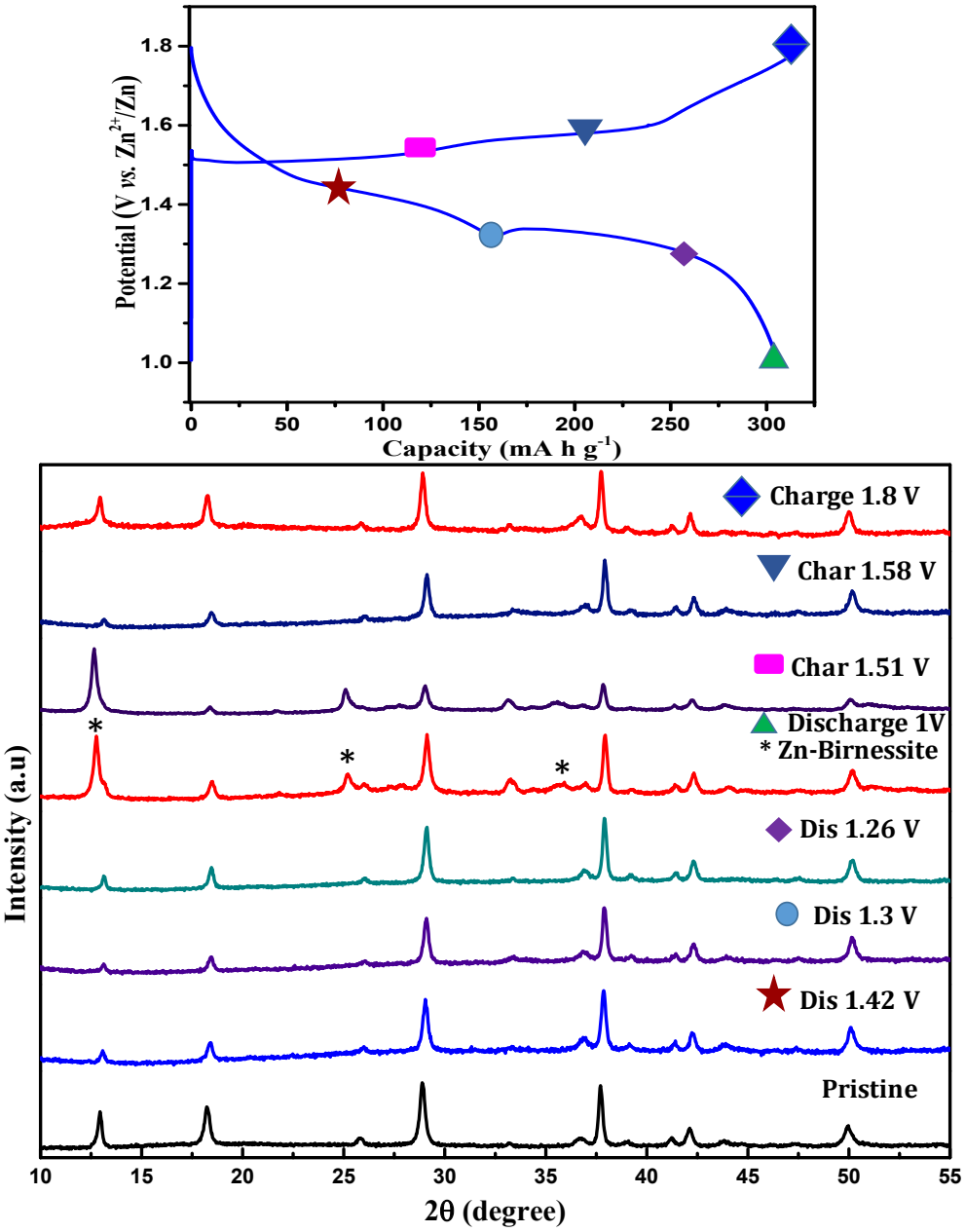

Figure S7: Ex situ XRD patterns of pristine cathode at different states of charge/discharge. During discharge and charge segments, structural transition (phase transformation) occurred after 1.26 V and 1.51 V respectively.

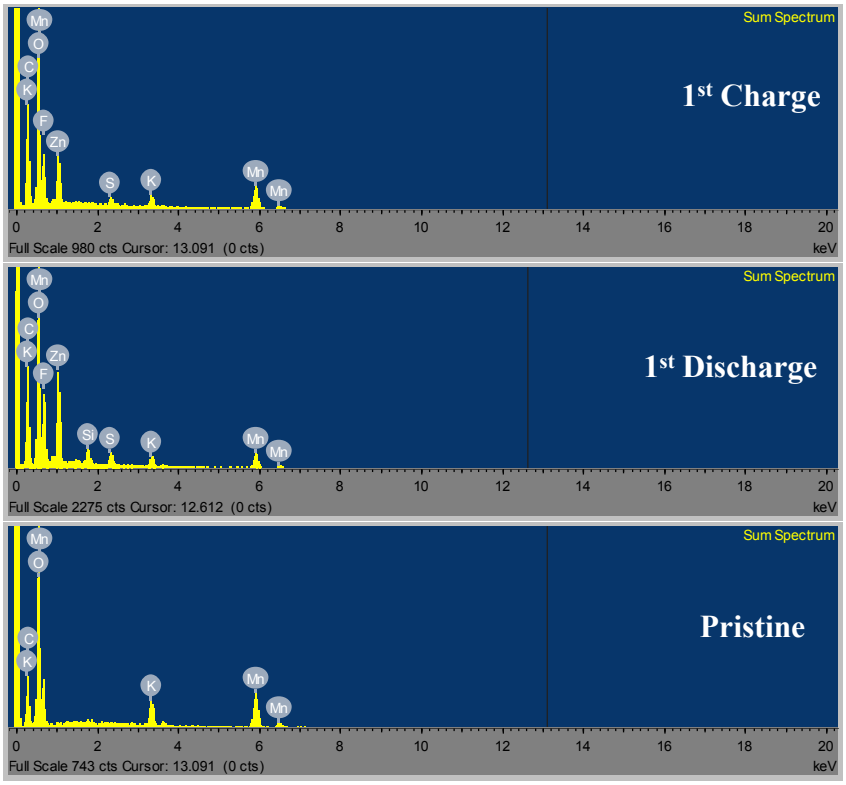

Figure S8: Comparative EDS spectra of pristine, 1st discharge and 1st charge electrodes.

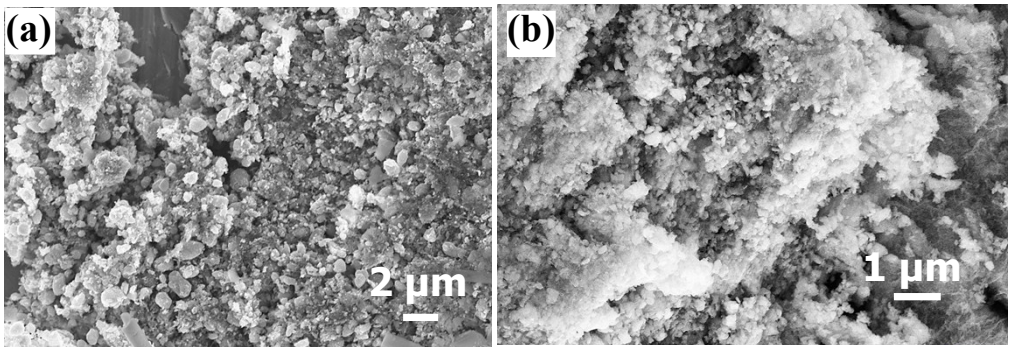

Figure S9: SEM images of the electrodes after (a) discharge and (b) charge showing the particles integrity. There is no significant morphological change upon battery cycling.

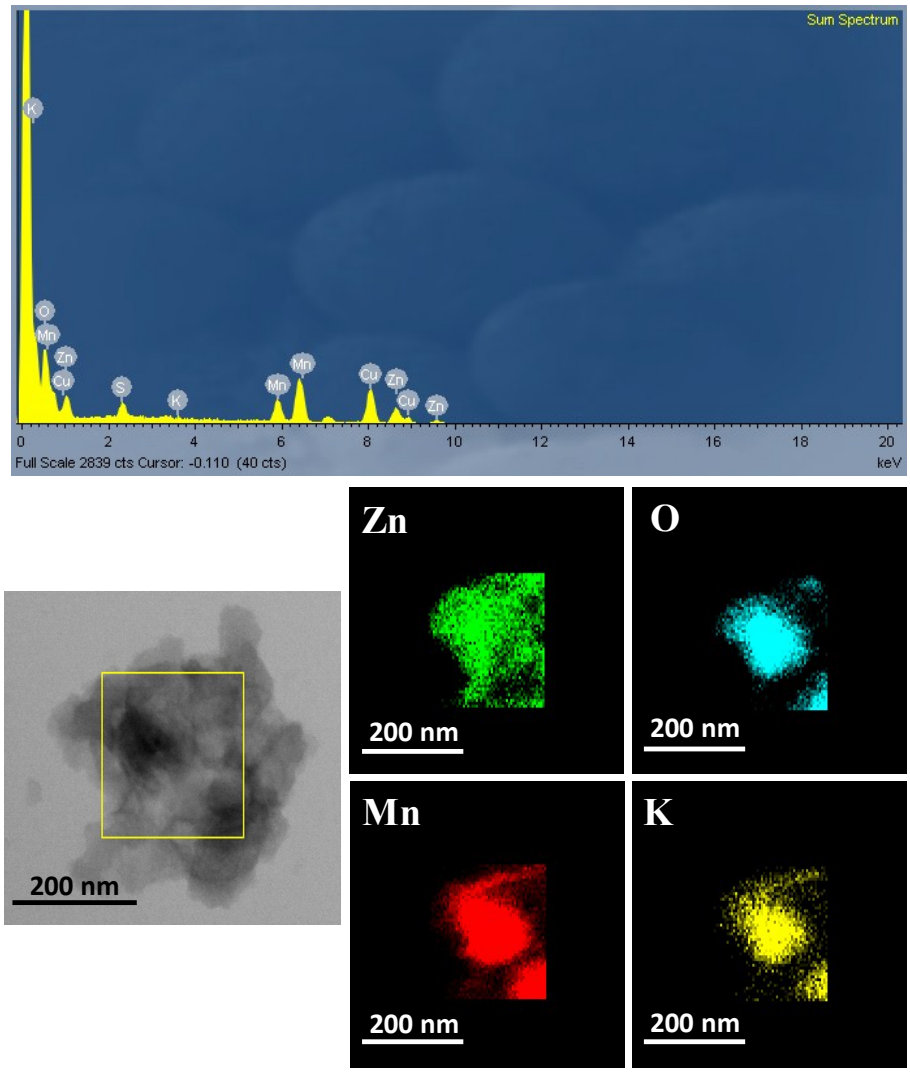

Figure S10: TEM analysis of 15th discharged electrode. Energy-dispersive X-ray microanalysis (EDS) and elemental mapping representing the particle showing the presence of the K-ion in the structure and uniform distribution of the all elements in the particles. Further, it confirmed integrity of the particles upon the multiple (dis)charge cycles.

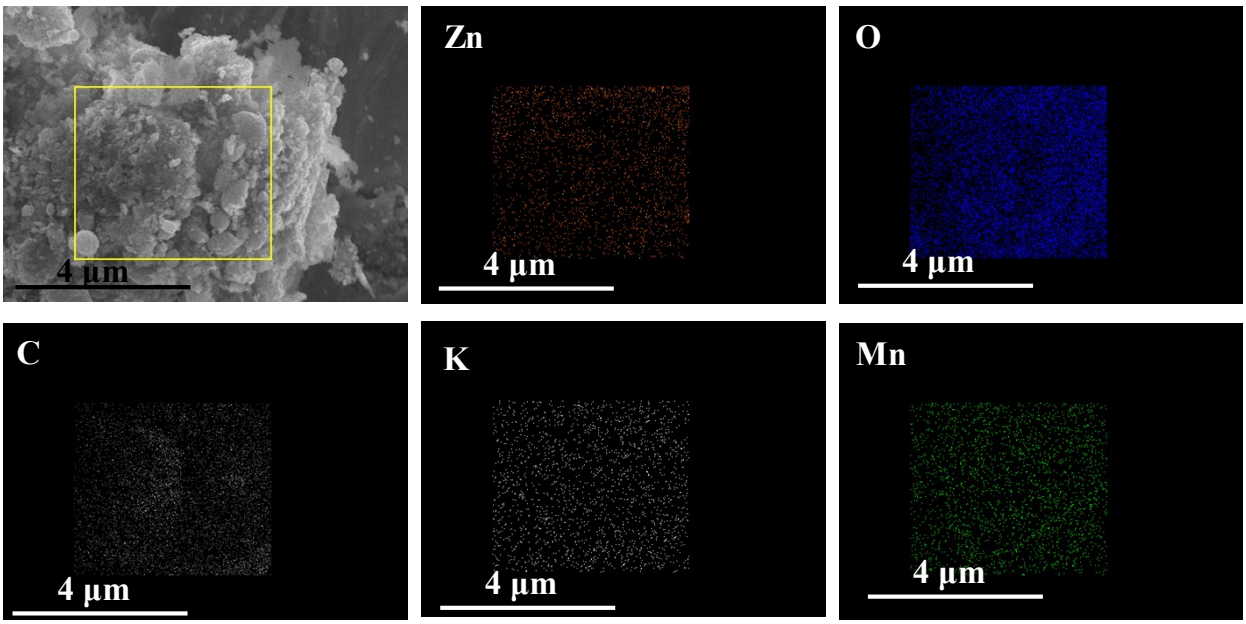

Figure S11: Elemental mapping of the discharged electrode.

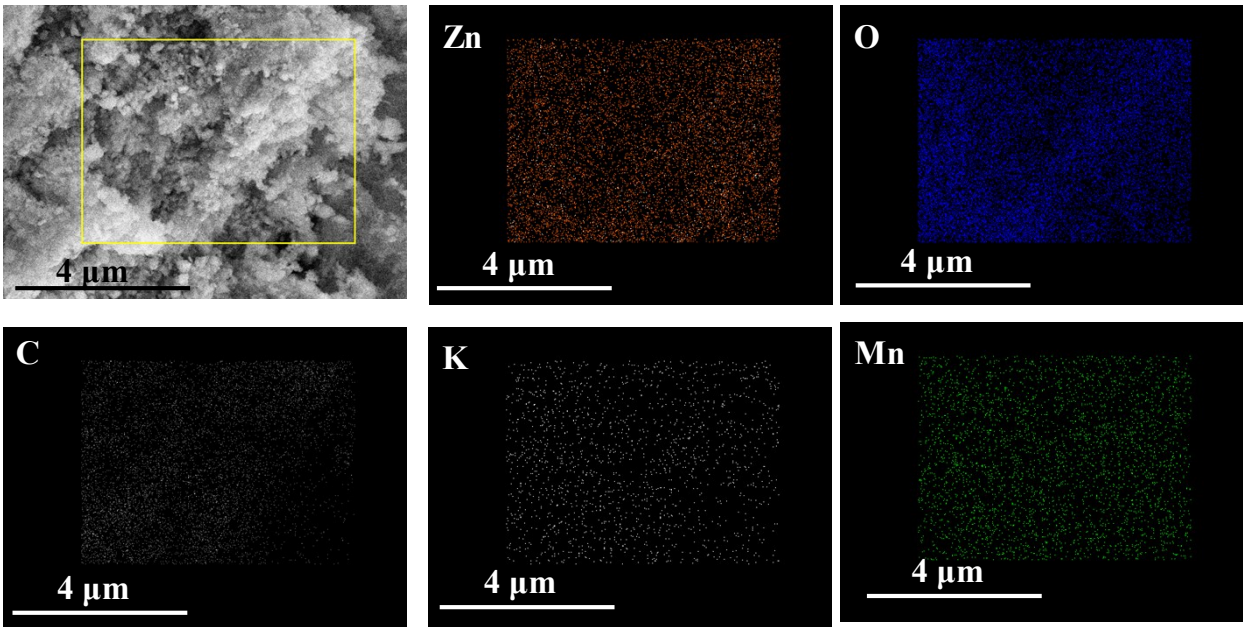

Figure S12: Elemental mapping of the charged electrode.

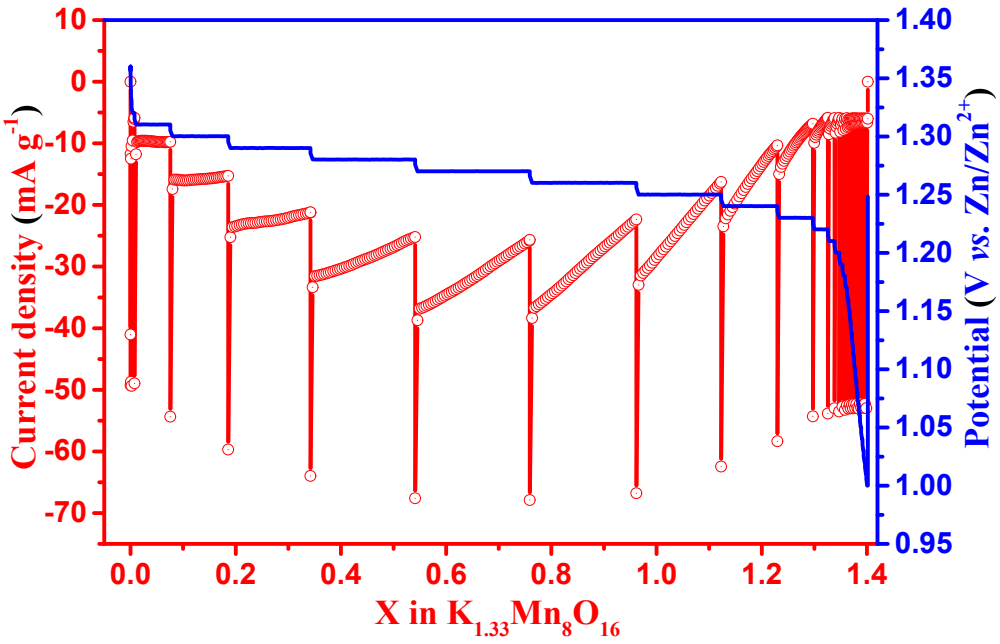

Figure S13: Potentiostatic intermittent titration (PITT) curve during the 1st discharge revealing the phase transformation with signature bell shape curve.

References:

1. H. Pan, Y. Shao, P. Yan, Y. Cheng, K. S. Han, Z. Nie, C. Wang, J. Yang, X. Li and P. Bhattacharya, *Nat. Energy*, 2016, **1**, 16039.
2. W. Sun, F. Wang, S. Hou, C. Yang, X. Fan, Z. Ma, T. Gao, F. Han, R. Hu and M. Zhu, *J. Am. Chem. Soc.*, 2017, **139**, 9775.
3. C. Xu, B. Li, H. Du and F. Kang, *Angew. Chem. Int. Ed.*, 2012, **124**, 957.
4. B. Lee, C. S. Yoon, H. R. Lee, K. Y. Chung, B. W. Cho and S. H. Oh, *Sci. Rep.*, 2014, 4, 6066.
5. M. H. Alfaruqi, J. Gim, S. Kim, J. Song, J. Jo, S. Kim, V. Mathew and J. Kim, *J. Power Sources*, 2015, **288**, 320.
6. I. Cui, X. Wu, S. Yang, C. Li, F. Tang, J. Chen, Y. Chen, Y. Xiang, X. Wu and Z. He, *Front. Chem.*, 2018, **6**, 352.